

# Selective Visible-Light-Driven CO<sub>2</sub> Reduction on a p-Type Dye-Sensitized NiO Photocathode

Andreas Bachmeier,<sup>†</sup> Samuel Hall,<sup>†</sup> Stephen W. Ragsdale,<sup>‡</sup> and Fraser A. Armstrong<sup>\*,†</sup>

<sup>†</sup>Inorganic Chemistry Laboratory, Department of Chemistry, University of Oxford, South Parks Road, Oxford OX1 3QR, Oxfordshire, United Kingdom

<sup>‡</sup>Department of Biological Chemistry, University of Michigan, Ann Arbor, Michigan 48109-0606, United States

**S** Supporting Information

**ABSTRACT:** We present a photocathode assembly for the visible-light-driven selective reduction of CO<sub>2</sub> to CO at potentials below the thermodynamic equilibrium in the dark. The photoelectrode comprises a porous p-type semiconducting NiO electrode modified with the visible-light-responsive organic dye P1 and the reversible CO<sub>2</sub> cycling enzyme carbon monoxide dehydrogenase. The direct electrochemistry of the enzymatic electrocatalyst on NiO shows that in the dark the electrocatalytic behavior is rectified toward CO oxidation, with the reactivity being governed by the carrier availability at the semiconductor–catalyst interface.

Converting solar energy into storable fuels is an important option for securing future renewable energy.<sup>1</sup> By no means a new concept – artificial photosynthesis (AP), unlike natural photosynthesis, is dedicated solely to efficient fuel formation and does not compete for untenable resources: it could work on urban rooftops.<sup>2</sup> The modern field is very much in its infancy, as many researchers strive, piece by piece, to learn and copy the tricks that biology has perfected. The hope is that important lessons from bench-level experiments will ultimately be taken up for development. As a general rule, AP-derived fuels can either be H<sub>2</sub>, the immediate product of water splitting, or carbon compounds such as methanol. Most obviously, carbon fuels can be formed indirectly by “hydrogenation” of CO<sub>2</sub>, similar to the processes occurring in photosynthetic dark reactions; but *direct* reduction of CO<sub>2</sub> is also an attractive possibility that could lead to CO<sub>2</sub> replacing petrochemicals as the feedstock for value-added organic chemicals. Like natural photosynthesis, AP can be broken down into four essential processes: harvesting of visible light, charge (electron–hole) separation, fuel formation, and water oxidation to O<sub>2</sub>; the last two processes require an efficient and selective catalyst. It is difficult to integrate all of these processes, so researchers have streamlined efforts by focusing on individual aspects.

We herein address the direct reduction of CO<sub>2</sub> to CO using a p-type semiconductor as a photocathode. Reductive CO<sub>2</sub> activation is a fundamentally challenging process, as the simple one-electron reduction to the CO<sub>2</sub><sup>•−</sup> radical anion ( $E = -1.9$  V vs SHE) is highly unfavorable. In contrast, synchronous proton-coupled two-electron reduction of CO<sub>2</sub> to CO or formate has no such energy-costing restriction.<sup>3</sup> Selectivity is also important.<sup>4,5</sup> With evolved active sites that are virtually perfect, it is no surprise

that enzymes lead the way, and carbon monoxide dehydrogenase or formate dehydrogenase are both established as reversible electrocatalysts for CO<sub>2</sub> cycling.<sup>6</sup> In a wider context, little is known about electron transfer between semiconductors and *reversible* electrocatalysts. The photoelectrochemical cell we now describe comprises a dye-sensitized p-type NiO cathode (P1–NiO) functionalized by spontaneous adsorption of carbon monoxide dehydrogenase I from *Carboxydotherrmus hydrogenoformans* (henceforth abbreviated as CODH) (Figure 1).

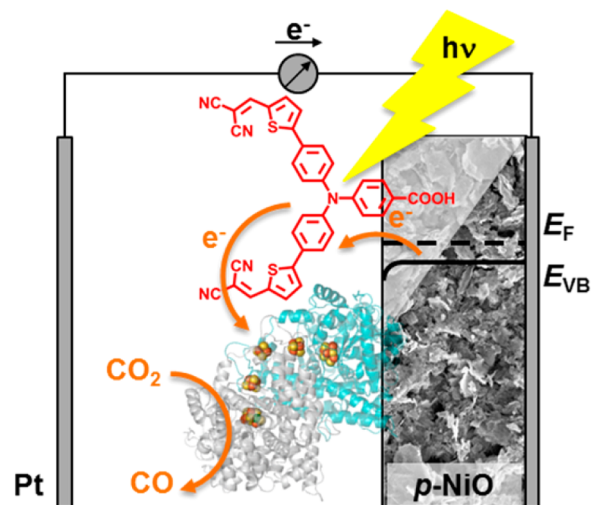


**Figure 1.** Scheme showing a photoelectrochemical cell for selective reduction of CO<sub>2</sub> to CO at p-type NiO. Light absorption by the organic dye P1 (red) is followed by electron transfer to CODH, which is coadsorbed on the NiO surface and carries out CO<sub>2</sub> reduction, while hole injection into the NiO valence band regenerates the P1 ground state. The porous nature of the NiO surface is indicated by the SEM image (the full image is given in the Supporting Information). The Fermi level and valence band potentials of NiO are denoted as  $E_F$  and  $E_{VB}$ .

Sun and co-workers introduced P1 as an organic photosensitizer for p-type dye-sensitized solar cells<sup>7</sup> and more recently achieved light-driven H<sub>2</sub> evolution by coadsorbing P1 and a molecular cobalt cobaloxime catalyst on NiO.<sup>8</sup> Taking their lead, we have adapted the concept for light-driven CO<sub>2</sub> reduction. The

Received: July 10, 2014

Published: September 19, 2014

mechanistic principle being exploited is that each excitation of P1 results in transfer of an electron to its coadsorbed partner CODH, passing through a relay of FeS clusters to the [Ni4Fe-4S] active site at which CO<sub>2</sub> is converted to CO in a two-electron proton-coupled electron transfer (PCET) reaction. Unlike simple molecular catalysts, enzymes such as CODH have a highly efficient active site as well as additional redox centers to capture, irreversibly,<sup>9</sup> more than enough reducing or oxidizing equivalents needed to complete the catalytic cycle. Following each electron-transfer step, the P1 ground state is regenerated through hole injection into the NiO valence band. The relevant electrochemical potentials of the individual components are given in Table 1.

**Table 1. Reduction Potentials of the Individual Components of the CO<sub>2</sub>-Reducing Photocathode Assembly<sup>a</sup>**

	$E(\text{CO}_2/\text{CO})$	$E(\text{P1}/\text{P1}^-)$	$E_{\text{VB}}, E_{\text{CB}}$
CODH	-0.46 <sup>3</sup>		
P1		-1.13 <sup>7,10</sup>	
NiO			0.60, -3.00 <sup>11</sup>

<sup>a</sup>All values in V vs SHE at pH 6.

First, we studied the dark electrocatalytic activity of CODH adsorbed on a p-type NiO electrode using protein film electrochemistry (PFE), a suite of techniques that provide important mechanistic information on redox enzymes under turnover conditions.<sup>12</sup> The turnover frequencies (TOFs) for CO<sub>2</sub> reduction and CO oxidation achieved with CODH are unmatched by any synthetic catalyst.<sup>13</sup>

When adsorbed on a pyrolytic graphite edge (PGE) electrode, CODH displays catalytic activity for both CO<sub>2</sub> reduction and CO oxidation (CO<sub>2</sub> and CO are bubbled through the solution as a 50/50 gas mixture), as shown in Figure 2A. Importantly, the cyclic voltammogram (CV) cuts sharply through the zero-current axis at the thermodynamic potential. The active site alternates between two catalytically active states  $C_{\text{red1}}$  and  $C_{\text{red2}}$  that are separated by two electrons (Scheme 1), with  $C_{\text{int}}$  as an intermediate formed during long-range electron transfers from the FeS clusters.

In contrast to the reversible catalytic interconversion of CO<sub>2</sub> and CO observed on the metallic-type PGE electrode, CODH behaves as a *unidirectional* CO oxidizer (Figure 2B, red trace) when attached to NiO; in other words, the otherwise bidirectional catalysis is rectified. Indeed, a catalytic oxidation current is observed only upon application of an overpotential of approximately 0.6 V. (Under such oxidizing conditions, CODH converts slowly to the inactive  $C_{\text{ox}}$  state<sup>14</sup>). To prove that the oxidation current stems from catalytic turnover, KCN was injected into the cell (to a final concentration of 10 mM; Figure 2B, blue voltammogram). Cyanide, which is isoelectronic with CO, targets the  $C_{\text{red1}}$  state of CODH (Scheme 1), thereby selectively inhibiting CO oxidation;<sup>14</sup> the voltammogram thus obtained resembles the baseline (bare NiO). The results mirror recent observations<sup>15</sup> with CODH adsorbed on the n-type materials TiO<sub>2</sub> and CdS, as illustrated in Figure 2C, which shows cyclic voltammograms of CODH adsorbed on TiO<sub>2</sub> recorded under conditions identical to those for the voltammograms displayed in Figure 2A,B. In contrast to p-NiO, CO oxidation at n-TiO<sub>2</sub> is barely detectable, whereas a strong reduction current is observed; this is established to be CO<sub>2</sub> reduction by the introduction of cyanate ( $\text{NCO}^-$ , isoelectronic with CO<sub>2</sub>), which

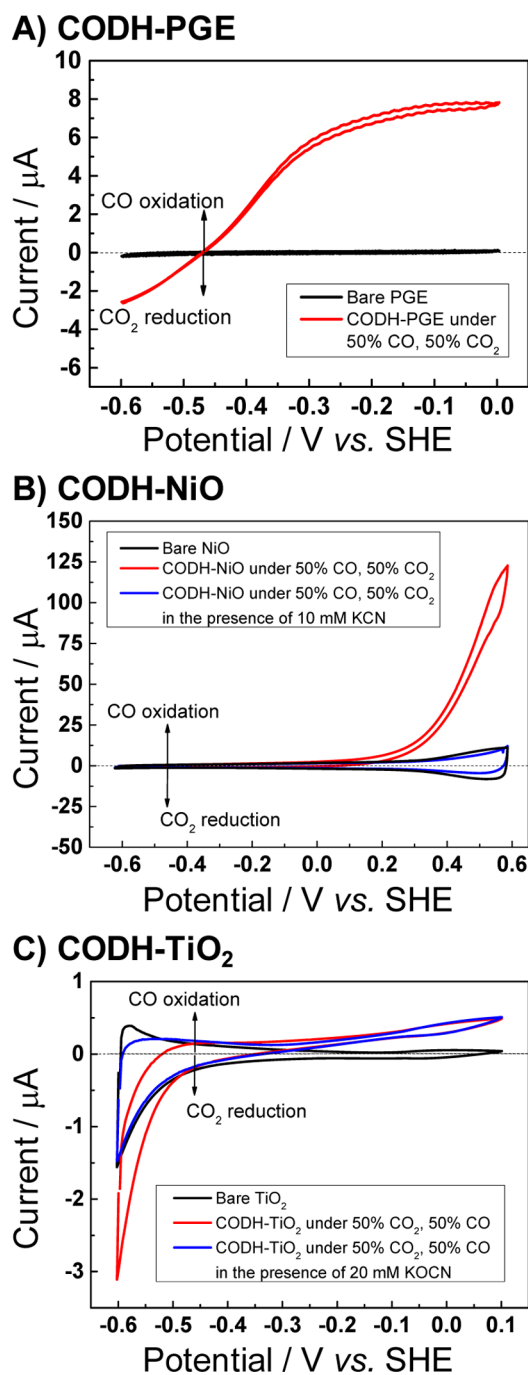
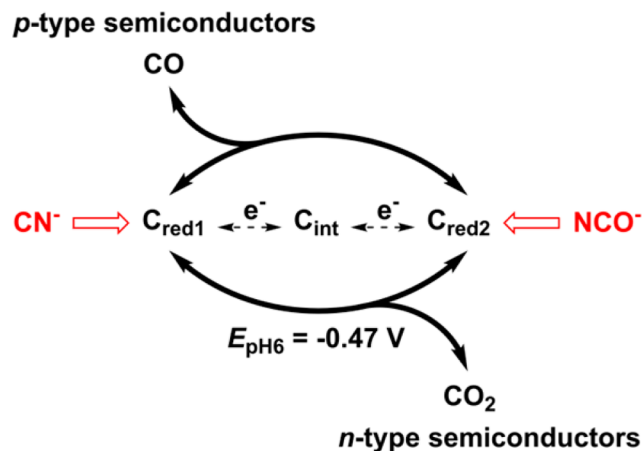


**Figure 2.** Cyclic voltammograms of CODH adsorbed on (A) PGE, (B) NiO, and (C) TiO<sub>2</sub>. Current–potential curves of the bare electrodes are depicted in black; experiments with adsorbed CODH (recorded with a 50% CO/50% CO<sub>2</sub> gas mixture bubbling through the cell) are shown in red. The blue CVs in (B) and (C) were recorded in the presence of 10 mM KCN (B) and 20 mM KOCN (C). Other conditions:  $T = 20^\circ\text{C}$ , 0.2 M MES buffer (pH 6), scan rate = 10 mV s<sup>-1</sup>. (A) and (C) are adapted from ref 15.

targets the  $C_{\text{red2}}$  state and blocks CO<sub>2</sub> reduction (see Scheme 1 and the blue trace in Figure 2C).

The results highlight the concept that the activity of an electrocatalyst attached to a semiconductor depends greatly on the properties of that semiconductor: the resulting rectification in either direction, depending on choice of semiconductor, is evident only when an electrocatalyst that otherwise behaves

**Scheme 1. Redox States<sup>a</sup> Involved in Catalytic CO<sub>2</sub> Interconversion at the Active Site of CODH and How p-Type and n-Type Semiconductors Rectify Catalytic Electron Flow**



<sup>a</sup> $C_{red1}$  and  $C_{red2}$  are the catalytically active states that effect CO oxidation and CO<sub>2</sub> reduction, respectively. The transient  $C_{int}$  state participates in the half-cycle regeneration of these active states. The small-molecule inhibitors CN<sup>-</sup> and NCO<sup>-</sup> selectively intercept states  $C_{red1}$  and  $C_{red2}$  and inhibit CO oxidation (CN<sup>-</sup>) and CO<sub>2</sub> reduction (NCO<sup>-</sup>).<sup>14</sup>

reversibly is used.<sup>15</sup> The surface concentration of the majority carriers in a semiconductor depends exponentially on the difference between the applied potential  $E$  and the flatband potential  $E_{fb}$ .<sup>16</sup> The catalytic directionality enforced on n-type TiO<sub>2</sub> coincides with a change in carrier availability around the flatband potential of the semiconductor [ $E_{fb}(\text{TiO}_2) \approx -0.50 \text{ V}$  vs SHE at pH 6].<sup>15</sup> In chemical terms, some Ti<sup>4+</sup> sites are reduced to Ti<sup>3+</sup>. In contrast, p-type NiO ( $E_{fb} \approx 0.61 \text{ V}$  vs SHE at pH 6)<sup>11</sup> forms a depletion layer at potentials negative of  $E_{fb}$ , which acts as a barrier for electron transfer from the semiconductor to the catalyst, blocking CO<sub>2</sub> reduction. As  $E_{fb}$  is approached, the conductivity of NiO increases exponentially, allowing CO oxidation catalysis to occur. In chemical terms, some Ni<sup>2+</sup> sites are oxidized to Ni<sup>3+</sup>. This effect is reflected in a steep increase in the catalytic oxidation current in Figure 2B positive of ca. 0.3 V vs SHE, i.e., relatively close to  $E_{fb}$ .

Having established the electroactivity of CODH on NiO, we sensitized the semiconductor with the visible-light-absorbing dye P1 [see the Supporting Information (SI) for experimental details]. The synthesis of P1 was carried out as described previously.<sup>7</sup> Figure 3 shows linear sweep voltammograms recorded under chopped illumination in CO<sub>2</sub>-saturated buffer (cyclic voltammograms of NiO–P1 are depicted in Figure S5 in the SI). Bare NiO shows very little photocurrent because of its large band gap of 3.6 eV (black current–potential curve). Upon sensitization with P1, the photocurrent increases, since P1 is capable of absorbing visible light ( $\lambda_{max} = 550 \text{ nm}$  in solution and 500 nm when adsorbed on NiO).<sup>7</sup> Modification with CODH results in a further photocurrent enhancement, which we ascribe (see below) to the light-driven reduction of CO<sub>2</sub>. Photoexcited P1 provides sufficient driving force to effect CO<sub>2</sub> reduction catalyzed by CODH (see Table 1) but does not reduce CO<sub>2</sub> itself. The LUMO of P1 lies ca. 0.7 V lower in energy than the CO<sub>2</sub>/CO<sub>2</sub><sup>•-</sup> redox couple: importantly, as a single-electron-transfer dye that is not capable of accumulating a second electron, P1 cannot undergo the PCET reactions that are required to

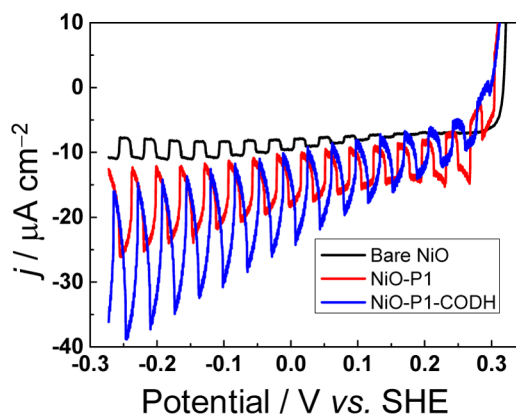


**Figure 3.** Linear sweep voltammograms of NiO (black), NiO–P1 (red), and NiO–P1–CODH (blue) recorded under chopped illumination (0.5 Hz, 45 mW cm<sup>-2</sup>) and CO<sub>2</sub> flow. Other conditions: 0.2 M MES buffer (pH 6),  $T = 32 \text{ }^\circ\text{C}$ , scan rate = 10 mV s<sup>-1</sup>.

lower the activation barrier for CO<sub>2</sub> activation, in contrast to CODH (which easily accumulates the two electrons needed).

To verify that the photocurrent enhancement we observed upon adsorption of CODH on NiO–P1 is due to catalytic conversion of CO<sub>2</sub> to CO, we once again used NCO<sup>-</sup> as a selective inhibitor of CO<sub>2</sub> reduction.<sup>17</sup> Figure 4A depicts transient photocurrents of NiO–P1–CODH recorded at  $-0.27 \text{ V}$  vs SHE (pH 6), which represents a 0.2 V underpotential with respect to CO<sub>2</sub> reduction in the dark. The photocurrent decreases significantly upon introduction of 60 mM KOCN, which establishes that the major proportion of the observed photocurrent stems from CO<sub>2</sub> reduction. Control experiments in the absence of CODH (i.e., NiO–P1 only) showed that injecting KOCN had no effect on the photocurrent (Figure S7).

Having identified the nature of the photocurrent, we assessed the stability of CO<sub>2</sub> reduction. Figure 4B depicts the temporal behavior of the catalytic current produced by NiO–P1–CODH during prolonged illumination (dark intervals are indicated by the letter “d”). The assembly shows good stability until cyanate is injected, analogous to the experiment depicted in Figure 4A, again demonstrating the catalytic turnover of the photocathode–catalyst system. Both Figures 3 and 4 strongly support a mechanism analogous to that described by Sun and co-workers for H<sub>2</sub> production.<sup>8</sup> In our system, P1 acts as a visible-light-responsive sensitizer that generates excited-state electrons, transfers these to CODH for catalysis, and is regenerated via hole injection into NiO.

In conclusion, catalytic electron flow through the CO<sub>2</sub>-reducing enzyme CODH, which behaves as a reversible catalyst on a metallic electrode, is rectified when CODH is attached to n-type (CO<sub>2</sub> reduction) or p-type (CO oxidation) semiconductors. When NiO is sensitized with the dye P1, a photocathode is produced that selectively reduces CO<sub>2</sub> to CO under visible-light illumination and application of a mildly reducing potential. The assembly shows good stability under turnover conditions, indicating that it could be coupled with a photoanode for water oxidation in a tandem photoelectrochemical cell to close the photosynthetic cycle. These experiments are currently in progress. Although not suitable for large-scale applications, reversible and highly selective electrocatalysts such as CODH are valuable model catalysts for AP. They serve as depolarizers that overcome the kinetic burden of sluggish catalysis and therefore allow the study of other mechanistic bottlenecks *in operando*. For example, rectification of catalytic electron transport at a



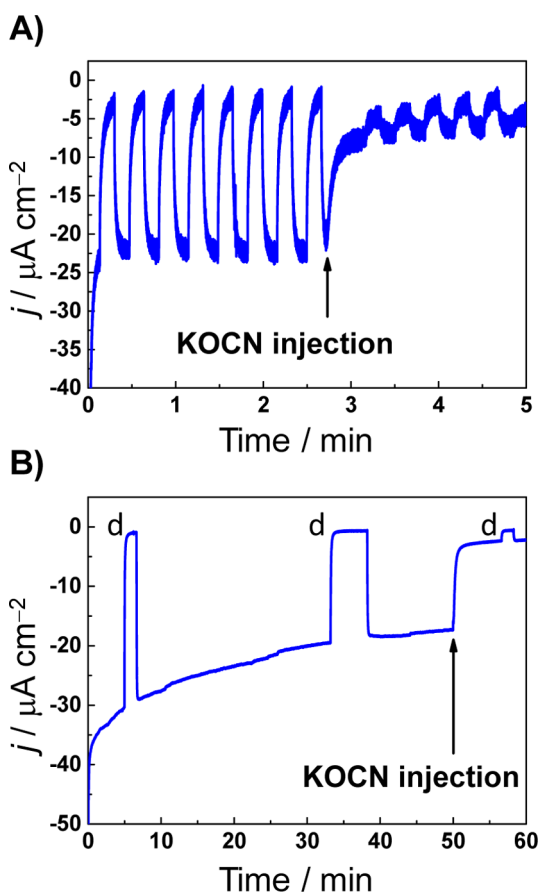


**Figure 4.** Chronoamperometry experiments on NiO–P1–CODH under a flow of CO<sub>2</sub> with the potential held at  $-0.27$  V vs SHE. Potassium cyanate (KOCN) was injected to a final concentration of 60 mM. (A) Transient photocurrents under chopped illumination. (B) Continuous illumination to assess the stability of the photocathode assembly under turnover conditions; “d” represents dark intervals. The experiments were carried out under white-light illumination ( $45 \text{ mW cm}^{-2}$ ) and CO<sub>2</sub> flow in 0.2 M MES buffer (pH 6) at  $T = 32$  °C.

semiconductor is revealed only by using a catalyst that is otherwise reversible. Multicentered enzymes, which have well-defined and stable active sites, have a special ability to accumulate electrons, a property that is less likely for simple catalysts but likely to be very important in competing with recombination.

## ■ ASSOCIATED CONTENT

### 📄 Supporting Information

Full materials and methods; NiO and P1 synthesis and characterization; electrode fabrication; (photo)electrochemical methods and equipment. This material is available free of charge via the Internet at <http://pubs.acs.org>.

## ■ AUTHOR INFORMATION

### Corresponding Author

fraser.armstrong@chem.ox.ac.uk

### Notes

The authors declare no competing financial interest.

## ■ ACKNOWLEDGMENTS

This research was supported by the Biological and Biotechnological Sciences Research Council (Grants BB/H003878-1, BB/I022309-1, and BB/L009722/1 to F.A.A.) and the Engineering

and Physical Sciences Research Council (Supergen V Grant EP/H019480/1 to F.A.A.). A.B. acknowledges St. John's College Oxford for a St. John's College Graduate Scholarship. F.A.A. is a Royal Society-Wolfson Research Merit Award holder. The authors thank Prof. Michael Hayward, Dr. Malcolm Stewart, and Prof. Jamie Warner for providing access to a high-temperature furnace, synthetic equipment, and SEM, respectively.

## ■ REFERENCES

- (1) Lewis, N. S.; Nocera, D. G. *Proc. Natl. Acad. Sci. U.S.A.* **2006**, *103*, 15729.
- (2) Ciamician, G. *Science* **1912**, *36*, 385.
- (3) Benson, E. E.; Kubiak, C. P.; Sathrum, A. J.; Smieja, J. M. *Chem. Soc. Rev.* **2009**, *38*, 89.
- (4) Zhu, W.; Michalsky, R.; Metin, Ö.; Lv, H.; Guo, S.; Wright, C. J.; Sun, X.; Peterson, A. A.; Sun, S. *J. Am. Chem. Soc.* **2013**, *135*, 16833.
- (5) Kumar, B.; Llorente, M.; Froehlich, J.; Dang, T.; Sathrum, A.; Kubiak, C. P. *Annu. Rev. Phys. Chem.* **2012**, *63*, 541.
- (6) Bachmeier, A.; Sirtanaratkul, B.; Armstrong, F. A. In *From Molecules to Materials—Pathways to Artificial Photosynthesis*; Rozhkova, E. A., Ariga, K., Eds.; Springer: in press.
- (7) Qin, P.; Zhu, H.; Edvinsson, T.; Boschloo, G.; Hagfeldt, A.; Sun, L. *J. Am. Chem. Soc.* **2008**, *130*, 8570.
- (8) Li, L.; Duan, L.; Wen, F.; Li, C.; Wang, M.; Hagfeldt, A.; Sun, L. *Chem. Commun.* **2012**, *48*, 988.
- (9) Wilker, M. B.; Shinopoulos, K. E.; Brown, K. A.; Mulder, D. W.; King, P. W.; Dukovic, G. *J. Am. Chem. Soc.* **2014**, *136*, 4316.
- (10) Qin, P.; Wiberg, J.; Gibson, E. A.; Linder, M.; Li, L.; Brinck, T.; Hagfeldt, A.; Albinsson, B.; Sun, L. *J. Phys. Chem. C* **2010**, *114*, 4738.
- (11) He, J.; Lindström, H.; Hagfeldt, A.; Lindquist, S.-E. *Sol. Energy Mater. Sol. Cells* **2000**, *62*, 265.
- (12) Vincent, K. A.; Parkin, A.; Armstrong, F. A. *Chem. Rev.* **2007**, *107*, 4366.
- (13) Can, M.; Armstrong, F. A.; Ragsdale, S. W. *Chem. Rev.* **2014**, *114*, 4149.
- (14) Wang, V. C. C.; Can, M.; Pierce, E.; Ragsdale, S. W.; Armstrong, F. A. *J. Am. Chem. Soc.* **2013**, *135*, 2198.
- (15) Bachmeier, A.; Wang, V. C. C.; Woolerton, T. W.; Bell, S.; Fontecilla-Camps, J. C.; Can, M.; Ragsdale, S. W.; Chaudhary, Y. S.; Armstrong, F. A. *J. Am. Chem. Soc.* **2013**, *135*, 15026.
- (16) Bard, A. J.; Faulkner, L. R. *Electrochemical Methods: Fundamentals and Applications*, 2nd ed.; John Wiley & Sons Inc.: New York, 2001.
- (17) Because of the minute amounts of enzymes on the electrode surface (pmol), even prolonged illumination over several hours did not produce enough CO to allow detection by gas chromatography (see Figure S6).